agronomy

MDPI

*Article*

# Prediction of Anthracnose Risk in Large-Leaf Tea Trees Based on the Atmospheric Environmental Changes in Yunnan Tea Gardens—Cox Regression Model and Machine Learning Model

**Rong Ye [1,2,†], Guoqi Shao [2,†], Zifei Ma [2], Quan Gao [3], Baijuan Wang [4] and Tong Li [2,3,*]**

[1] College of Food Science and Technology, Yunnan Agricultural University, Kunming 650201, China; 15912913557@163.com
[2] The Key Laboratory for Crop Production and Smart Agriculture of Yunnan Province, Yunnan Agricultural University, Kunming 650201, China; 15751769522@163.com (G.S.); mzf@ynau.edu.cn (Z.M.)
[3] College of Big Data, Yunnan Agricultural University, Kunming 650201, China; gaoq@ynau.edu.cn
[4] College of Tea Science, Yunnan Agricultural University, Kunming 650201, China; wangbaijuan2023@163.com
* Correspondence: tli@ynu.edu.cn
† These authors contributed equally to this work.

**Abstract:** Crop diseases pose a major threat to agricultural production, quality, and sustainable development, highlighting the importance of early disease risk prediction for effective disease control. Tea anthracnose can easily occur in Yunnan under high-temperature and high-humidity environments, which seriously affects the ecosystem of tea gardens. Therefore, the establishment of accurate, non-destructive, and rapid prediction models has a positive impact on the conservation of biodiversity in tea plantations. Because of the linear relationship between disease occurrence and environmental conditions, the growing environmental conditions can be effectively used to predict crop diseases. Based on the climate data collected by Internet of Things devices, this study uses LASSO-COX-NOMOGRAM to analyze the expression of tea anthracrum to different degrees through Limma difference analysis, and it combines Cox single-factor analysis to study the influence mechanism of climate and environmental change on tea anthracrum. Modeling factors were screened by LASSO regression, 10-fold cross-validation and Cox multi-factor analysis were used to establish the basis of the model, the nomogram prediction model was constructed, and a Shiny- and DynNOM-visualized prediction system was built. The experimental results showed that the AUC values of the model were 0.745 and 0.731 in the training set and 0.75 and 0.747 in the verification set, respectively, when the predicted change in tea anthracnose disease risk was greater than 30% and 60%, and the calibration curve was in good agreement with the ideal curve. The accuracy of external verification was 83.3% for predicting tea anthracnose of different degrees. At the same time, compared with the traditional prediction method, the method is not affected by the difference in leaf background, which provides research potential for early prevention and phenotypic analysis, and also provides an effective means for tea disease identification and harm analysis.

**Keywords:** tea anthracnose; lasso; machine learning; prediction model; calibration curve; nomogram

check for updates

**Citation:** Ye, R.; Shao, G.; Ma, Z.; Gao, Q.; Wang, B.; Li, T. Prediction of Anthracnose Risk in Large-Leaf Tea Trees Based on the Atmospheric Environmental Changes in Yunnan Tea Gardens—Cox Regression Model and Machine Learning Model. *Agronomy* **2024**, *14*, 1501. https://doi.org/10.3390/agronomy14071501

Academic Editor: Sara Álvarez

Received: 15 June 2024
Revised: 5 July 2024
Accepted: 8 July 2024
Published: 10 July 2024

**Copyright:** © 2024 by the authors. Licensee MDPI, Basel, Switzerland. This article is an open access article distributed under the terms and conditions of the Creative Commons Attribution (CC BY) license (https://creativecommons.org/licenses/by/4.0/).

## 1. Introduction

Yunnan, known as the world's largest origin center and genetic diversity center of tea tree resources, boasts a vast distribution of ancient tea tree resources in numerous regions. As a result, Yunnan possesses rich tea tree resources. Tea cultivation is widespread due to its high nutritional and economic value [1]. However, the relatively low tea yield necessitates large-scale plantations. The timely detection and treatment of tea diseases is crucial, as transmission can lead to immeasurable losses. Unfortunately, the current process is time-consuming, laborious, and prone to misjudgment, subjective error, and variability [2–5]. To address this, information technology-based detection methods are increasingly employed for the accurate prediction of crop growth [6–10].

China, being a significant producer of agricultural products, places great importance on tea, which is susceptible to tea anthracnose, a common leaf disease widely distributed across tea-producing areas [11–13]. With more than 130 types of tea tree diseases in China, the annual reduction in tea production by 10–20% due to these diseases severely impacts tea quality. Therefore, early prediction following disease detection plays a vital role in ensuring tea production. In light of global climate change, tea tree diseases are becoming more prevalent, leading to the rapid development of computer vision methods based on tea disease characteristics. However, no cure or damage control for crops currently exists. Hence, there is an urgent need to predict the probability of disease occurrence and proactively devise solutions before significant damage is incurred.

Currently, scholars have made predictions about the growth model, physical and chemical composition, and incidence probability of tea by considering various factors such as the environment and soil. These predictions involve the use of soil physical and chemical properties, temperature, and environmental factors to anticipate physiological changes in crops [14–17]. One effective mathematical model for prediction is a nomogram, which combines multiple factors to forecast a specific outcome. Unlike other models, a nomogram presents results in a graphical format, enhancing its intuitiveness. Moreover, it is quick to construct and does not require a large amount of training data. However, while nomograms are commonly used in the medical field, their application in agronomy is relatively limited. To promote sustainable agricultural development and improve crop disease prediction, we aim to further explore and apply the use of nomograms in the agricultural field.

In order to counteract the disease effects of environmental stresses, including climate change and biodiversity, most crops exhibit a range of physiological and biochemical responses. This study proposes a tea anthracnose disease prediction model that directly perceives changes in climate and environmental conditions. By monitoring real-time changes in tea growing environmental conditions, this model accurately predicts the occurrence probability of tea anthracnose. The key environmental conditions considered in this model include air humidity, rainfall, light intensity, soil moisture content, carbon dioxide concentration, TBQ radiation value, and other factors. Based on these considerations, the researchers established the LASSO-COX-NOMOGRAM tea anthracnose disease risk prediction model. This model predicts the occurrence probability of tea growth diseases within a certain period by taking into account real-time changes in environmental conditions. The primary focus is on the effects of environmental factors such as air humidity, rainfall, light intensity, soil moisture content, carbon dioxide concentration, and TBQ radiation value on the occurrence of the disease. During the research process, environmental change data from the Yuecheng Base in Xishuangbanna Prefecture, Yunnan Province, in 2023 were collected through Internet of Things devices. These data facilitated the external verification of the tea lesion risk prediction model.

Based on Cox regression and machine learning, the risk degree prediction model of tea anthracnose was established in the Yuecheng Base of Xishuangbanna Prefecture, Yunnan Province. This model takes into account the comprehensive impact of environmental changes on the occurrence of tea anthracnose. By providing data predictions and model support, this research lays the foundation for further investigations into the effects of abiotic stress on tea anthracnose. Furthermore, the predictive capabilities of this model can be utilized to inform decision making in the management of tea gardens, enabling intelligent and proactive measures to prevent and control tea anthracnose outbreaks. This research has significant implications for the intelligent construction of tea gardens in specific regions of Yunnan and serves as a valuable tool for ongoing studies on the impact of abiotic stress on tea anthracnose.

## 2. Materials and Methods

### *2.1. Overview of the Research Region*

The experimental research was conducted at the No. 1 base of Yuecheng Co., Ltd. (100° E, 21° N), in Xishuangbanna Prefecture, Yunnan Province, China—the birthplace of big-leaf

tea. This research focused on the most severe anthracnose disease. The area belongs to the tropical monsoon climate region. The region is located in the southwest monsoon climate zone, with an average daily temperature of 22 °C, a high effective accumulated temperature of 8761 °C, an annual average relative humidity of 79%, an annual average rainfall of 1665 mm, and an annual runoff of 700 mm. The tea garden, where this research took place, is a strip-planted tea garden on a slope. It mainly consists of Mengku large-leaf tea trees that are approximately 10 years old, providing 90% coverage. The region experiences a warm and humid climate throughout the year, with distinct seasons. The dry season occurs from November to February, while the rainy season is from June to August, making it an ideal environment for cultivating various teas. Surrounded by mountains and enveloped in high mountain clouds and mist, the area has rich organic matter in the soil, strong solar radiation, and frequent rainy days, which creates conditions for tea anthracnose to occur year-round. The disease is most prevalent in autumn and poses a significant threat to the genetic diversity of tea varieties. Figure 1 illustrates the tea garden.




**Figure 1.** Tea mountain photo.

The environmental monitoring system comprises an ecological simulation box, Alibaba Cloud server, and monitoring equipment. The ecological simulation box is equipped with sensors for air temperature and humidity, soil temperature and humidity, and temperature and humidity control. The collected data are uploaded to the Alibaba Cloud server via Wi-Fi connection through the router. The cloud server uses the MQTT protocol to receive, parse, and store data, and integrates field-side data into an intelligent data model for easy monitoring and learning. Subsequently, the data are transmitted to the end device via the MQTT protocol. Authorized users at the terminal can monitor data, adjust parameters, and perform remote control through computers and APP programs. Table 1 presents the parameters of the IoT sensors.

**Table 1.** The parameters of the IoT sensors.

| Sensor Type | Model Number | Range | Resolution | Precision |
|---|---|---|---|---|
| soil moisture sensor | DS18B20 | 0–100%RH | 0.1%RH | ±5% (53–100%) |
| light intensity sensor | RS-WS-4G-C5 | 0–20 W Lux | 1 Lux | ±5% |
| air temperature sensor | SS8050 | −40–80 °C | 0.1 °C | ≤0.1 °C |
| air humidity sensor | AHT10 | 0–100% RH | 0.1% RH | ≤0.1% RH |
| carbon dioxide sensor | SGA-900 | 0–10,000 ppm | 1 ppm | ±100 ppm |
| TBQ total radiation sensor | TBQ-2-B | 0–4000 W/m$^2$ | 0.1 W/m$^2$ | <±2% |

### *2.2. Identification and Occurrence Rules of Tea Anthracnose Symptoms*

In Yunnan, tea anthracnose is a highly prevalent disease in tea gardens, primarily affecting adult leaves but also old and young leaves. The disease initially presents itself as dark green water-stained spots on the tips or edges of the leaves. Over time, these spots expand and form yellow-brown irregular shapes along the leaf veins, with a clear boundary between the diseased area and the healthy part [7,18]. Subsequently, gray-white patches with small black spots, known as conidia, appear on the affected area. The leaves affected by the disease have a brittle texture and are prone to cracking, eventually leading to their detachment. In severe cases, tea gardens may experience a significant loss of tea leaves.

### *2.3. Preliminary Exploration of Environmental Influencing Factors of Anthracnose in Tea*

The occurrence of diseases is influenced by various factors, including environmental and climatic conditions, cultivation management, and plant varieties. In this study, tests were conducted on Colletotrichum strains of large-leaf tea in Mengku to determine the optimal conditions for temperature, pH, humidity, light intensity, soil environment, and altitude. These factors were found to affect the germination rate of colonies and spores.

Relevant physical and chemical composition detection experiments were conducted at the Yunnan organic tea industry Intelligent Engineering Research Center. Tea Colletotrichum strain C6 was obtained by isolating single spores from tea Colletotrichum diseased leaves. The strain was then cultured on a slant in a PDA test tube and stored in a 4 °C refrigerator [19,20]. A temperature gradient of 10 °C, 15 °C, 20 °C, 25 °C, 30 °C, and 35 °C was used. Culturing at 25 °C until the mycelium did not cover the Petri dish, hyphae were obtained from the edge of the colony and lines were drawn using the cross method. This process was repeated 5 times for each temperature, and the samples were placed in a 25 °C incubator for cultivation. After 48 h, the diameter of the colony was measured until the Petri dish was full. The pH was adjusted to five gradients (4, 5, 6, 7, and 8) using sterilized KCl-HCl and $Na_2HPO_4$-NaOH buffer solutions. The humidity was controlled by the germination rate of spores in distilled water, ranging from 80% to 100%. For soil collection, two points in alternate rows in the tea garden were randomly selected as fixed-point investigation areas. The topsoil (5 cm depth) from the soil surface to the cultivated layer soil within 25 cm was excavated. The altitude and light intensity were set to 5 intensities (2 Lux, 4 Lux, 6 Lux, 8 Lux, and 10 Lux) according to different periods. The experimental results are shown in Figure 2.

According to Figure 2, the preliminary exploration revealed that tea anthracnose colonies exhibited the fastest growth at a temperature of 25 °C and a pH of 6. This suggests that 25 °C is the most suitable temperature for its growth, and pH = 6 represents a neutral to slightly alkaline environment. However, it is important to note that the germination rate remains high even under mild or slightly acidic conditions. This can be attributed to the mild and humid climate of the Banna area throughout the year, as well as the dominance of Acidobacteria in the soil microbial community, which facilitates the rapid growth and development of tea anthracnose colonies [21]. The growth of the bacterial community and spore germination, on the other hand, are minimally influenced by different light conditions. The optimal temperature for spore germination is found to be 25 °C, with higher germination rates observed at lower temperatures compared to higher temperatures.

Additionally, a high germination rate is only achieved when the air humidity exceeds 95%, indicating that the rainy season is favorable for tea anthracnose spore germination. As for mycelial growth and sporulation, the most favorable temperature range is between 26 °C and 28 °C. Beyond 36 °C, mycelial growth ceases [22,23]. In addition, a small amount of tea anthracnose was detected in the soil in the data collection area of this study.

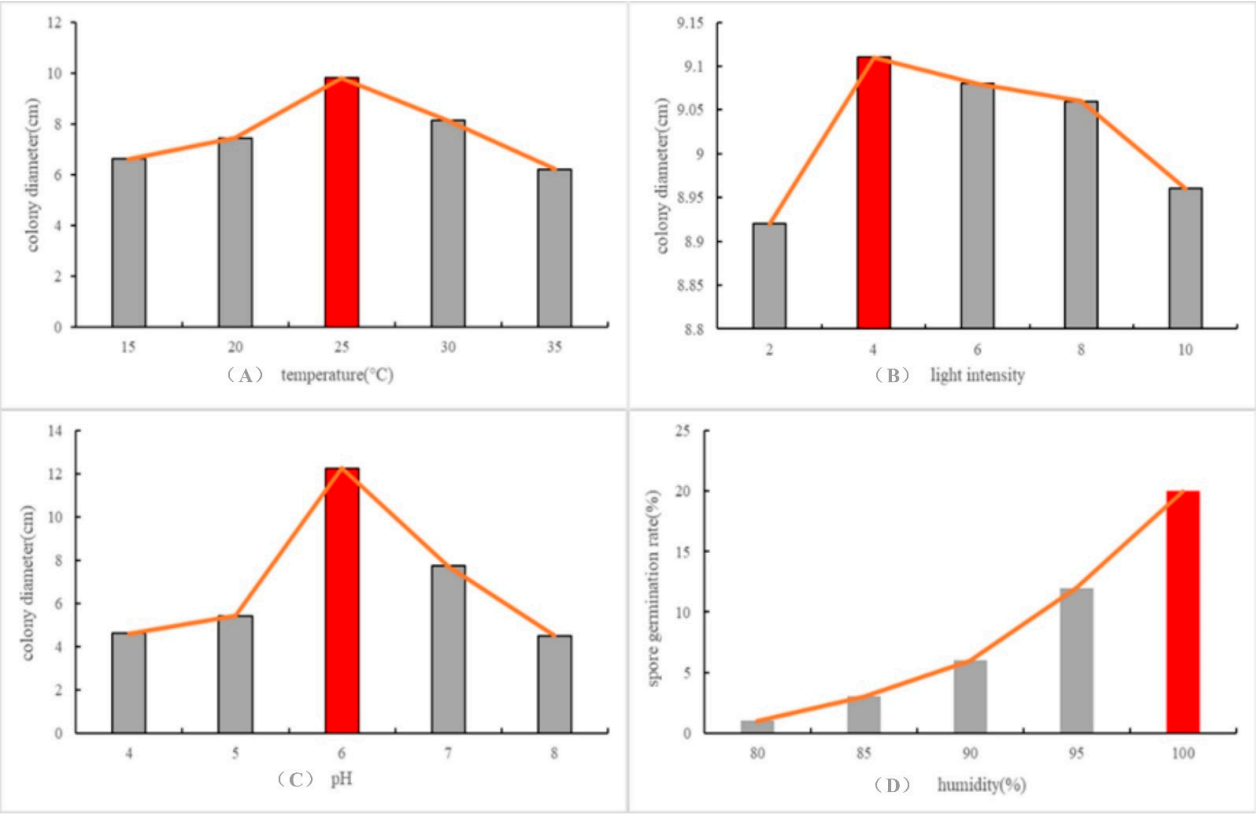


**Figure 2.** Effects of different environmental conditions on the colonies and spores of anthracnose bacteria in tea.

Spores typically invade the hairs on the back of young leaves, germinate, and produce germ tubes. In harsh environments, they can remain attached to the back of the leaves for up to 5 months. When conditions become favorable, they then invade the host and form small water-soaked lesions after an incubation period of approximately 1 week. These lesions gradually expand into irregular brown lesions. In this stage, the infected young leaves have matured into old leaves. Therefore, this study focuses on analyzing the environmental data within 7 days of the onset of illness. We calculate the average value, change difference, and change floating value for each indicator. By comparing these values, we can understand the differences at each time point and analyze the changing trend in a specific variable. This analysis helps researchers gain a better understanding of the data, make informed decisions, and predict future changing trends and risks. Ultimately, this study aims to develop a more accurate tea anthracnose disease prediction model.

### *2.4. Classification of Leaf Disease Degree*

The degree of leaf disease is categorized into three levels based on the proportion of the infected area compared to the whole leaf. Level 1 is considered mild, with an infection range of 0–30%. Level 2 is classified as moderate, with an infection range of 30–60%. Level 3 indicates a severe condition, with an infection range greater than 60%.

### *2.5. Statistical Analysis*

This study utilized an NVIDIA GeForce RTX 3060 GPU and a computer with 32 GB of memory. The CUDA11.1 version of the dependent library was used, along with R language version 4.1.2. In this study, the objective task was to make short-term predictions of tea anthracnose disease. In addition, 300 sets of climate change data were randomly selected from the Yunnan Province Xishuangbanna Dai Autonomous Prefecture Mengla Base for the years 2021–2023 for analysis, with 240 sets for the training set and 60 sets for the validation set. To address the limitation of insufficient modeling datasets, the Bootstrap method was further introduced to expand the dataset and enhance prediction accuracy and model precision. Data analysis was performed using SPSS 25.0 statistical software. The comparison between groups was conducted using the Chi-square test, while the Ridit test was used for grade data. Measurement data are expressed as the mean ± standard deviation, and the *t*-test was employed for group comparisons. Significant variables identified through single-factor analysis were included in the multi-factor analysis. LASSO-COX regression analysis was conducted, with a significance level of $p < 0.05$ indicating a statistically significant difference. Disease incidence statistics were performed, and both single-factor and Lasso analysis were employed to screen factors influencing the incidence of tea anthracnose. An influencing-factor-based nomogram prediction model was developed, and its prediction efficiency was analyzed using the ROC curve. The prediction reliability was expressed by the AUC, and the DeLong test was employed to compare AUC values between different schemes. To address the limitations of a small modeling dataset, the Bootstrap method (B = 1000) was introduced for internal verification, evaluating the model's accuracy and stability. Additionally, a calibration curve was drawn to assess the prediction effect of the model. Decision Curve Analysis (DCA) was utilized to evaluate the prediction efficiency and applicability of the model.

## 3. Results and Analysis

### *3.1. Single-Factor Logistic Regression Analysis*

Cox regression is a flexible and powerful statistical model, which is generally used to predict patient risk factor screening analysis in clinical medicine. It allows for the assessment of multiple risk factors simultaneously, without assuming any interactions between them. In this study, Equation (1) [24–26] is used to assess the collective influence of various environmental factors on the development of tea anthracnose disease.

$$h(t) = h_0(t)exp(\beta_1 x_1 + \cdots \beta_j x_j) \quad (1)$$

where $h(t)$ represents the disease risk function, which varies with different environmental factors. $h_0(t)$ is the intercept of the regression equation. $x_1$, $x_2 \cdots$, $x_j$ represent the independent variables, and $\beta_1$, $\beta_2 \cdots$, $\beta_j$ represent the regression coefficients.

To minimize the impact of data samples on model performance, this study randomly divided the dataset into training sets and validation sets in an 8:2 ratio. Using the Cox regression model, a single-factor comparative analysis was conducted on 30 variables that may affect disease changes. The analysis results are presented in Table 2. Among these, the selection of significant correlation factors ($p < 0.05$) indicates a strong correlation with tea lesions.

The analysis results in Table 2 indicate that there are 21 environmental factors significantly associated with tea diseases ($p < 0.05$). These factors include light intensity, humidity, temperature, carbon dioxide concentration, TBQ radiation value, and soil moisture, among others, as discussed in this article. These findings align with the preliminary exploration results presented in Section 2.3. Furthermore, in the single-factor analysis results, it was observed that more than 80% of the environmental factors ($p < 0.01$) contribute to the worsening of the disease. These environmental factors serve as initial predictors of the disease. Moving forward, we delve into more specific factors that influence disease progression, focusing on environmental factors.

**Table 2.** Univariate analysis results on the degree of variation in tea anthracnose disease.

| Significant Environmental Correlation Factors | HR | CI | *p* |
|---|---|---|---|
| Average light intensity (A1.W) | 1.05 | 1.04–1.08 | 0.044 |
| Average light intensity (A2.W) | 1.02 | 1.01–1.05 | 0.02 |
| Maximum temperature (A1.W) | 0.94 | 0.92–0.99 | 0.014 |
| Minimum temperature (A1.W) | 0.96 | 0.94–0.99 | 0.014 |
| Average temperature (A1.W) | 0.95 | 0.92–0.99 | 0.044 |
| Average night temperature (A1.W) | 1.05 | 1.02–1.09 | 0.025 |
| Maximum air humidity (A2.W) | 1.02 | 1.01–1.03 | 0.002 |
| Average relative humidity (A1.W) | 1.01 | 0.98–1 | 0.039 |
| Average relative humidity (A2.W) | 1.01 | 1–1.02 | 0.003 |
| Average daytime mean air humidity difference (A2.W) | 1.01 | 1–1.02 | 0.011 |
| Average daytime mean air humidity (A2.W) | 1.02 | 1.01–1.03 | 0.005 |
| Average daytime mean air humidity (A3.W) | 1.01 | 1–1.02 | 0.04 |
| Average night air humidity (A2.W) | 1.02 | 1.01–1.03 | 0.005 |
| Average night air humidity (A3.W) | 1.01 | 1–1.02 | 0.04 |
| Average $CO_2$ concentration (A2.W) | 1.01 | 1–1.02 | 0.049 |
| Daily mean $CO_2$ concentration (A2.W) | 1.01 | 1–1.02 | 0.019 |
| Average nocturnal $CO_2$ concentration (A3.W) | 1.02 | 1.01–1.03 | 0.019 |
| Mean total TPQ radiation (A2.W) | 0.98 | 0.97–0.99 | 0.018 |
| Maximum soil moisture content (A2.W) | 1.04 | 1.03–1.07 | 0.044 |
| $CO_2$ concentration difference (A1.W) | 1.02 | 1.01–1.04 | 0.05 |

Note. A1: mean value; A2: change difference; A3: change in floating value; W: 7 days; HR: Hazard Ratio; CI: Confidence Interval.

### *3.2. Differential Correlation Analysis*

This study analyzed the differences between the three grades of tea anthracnose lesions in Section 2.4 and the changes in environmental factors in the following week. Limma was used for screening with a significance level of $p < 0.05$ and a fold change of $|\log FC| \geq 1$. The results are shown in Figure 3A–C and Table 3.

**Table 3.** Statistics of the results of the difference analysis.

| Disease Severity Level | Overall Differential Expression Factors/Terms | Rising Factors/Terms | Decrease Factors/Terms |
|---|---|---|---|
| Mild Disease Risk prediction | 29 | 18 | 11 |
| Moderate Disease Risk Prediction | 19 | 13 | 6 |
| Severe Disease Risk Prediction | 11 | 7 | 4 |

As depicted in Figure 3, the tea anthracnose leaf, which progressed from a mild to severe disease within 7 days after the lesion occurred, was collected. It was observed that various environmental factors, including light intensity, TBQ radiation value, air humidity, carbon dioxide concentration, and soil humidity, exhibited a significant differential expression. During the disease progression cycle, higher concentrations of $CO_2$ were observed, along with a higher daytime air humidity and suitable light intensity. Furthermore, there was a greater difference in TBQ radiation intensity and soil moisture between morning and evening. Research indicates that increased $CO_2$ concentration and high light intensity cause changes in the chlorophyll and oxygen-containing water within the leaves, leading to a slowdown in internal reactions and alterations in the tea cell structure. Additionally, a strong TBQ radiation intensity inhibits the growth of tea anthracnose mycelia and spore germination, with high concentrations causing mycelia and spore distortion. The severity of tea lesions increases with the presence of suitable soil moisture, which facilitates the spread of disease spores. Moreover, the leaves located around the edge of the tea canopy are more susceptible to exposure to tea anthracnose fungi, thereby exacerbating the disease.

The results presented in Figure 4 demonstrate that the transition from mild risk to moderate risk in tea anthracnose is primarily influenced by TBQ radiation intensity. On the other hand, when transitioning from moderate risk to severe risk, factors such as soil

moisture and average $CO_2$ concentration play a significant role. Within the severe risk range, temperature emerges as the most crucial factor contributing to the worsening of the disease.

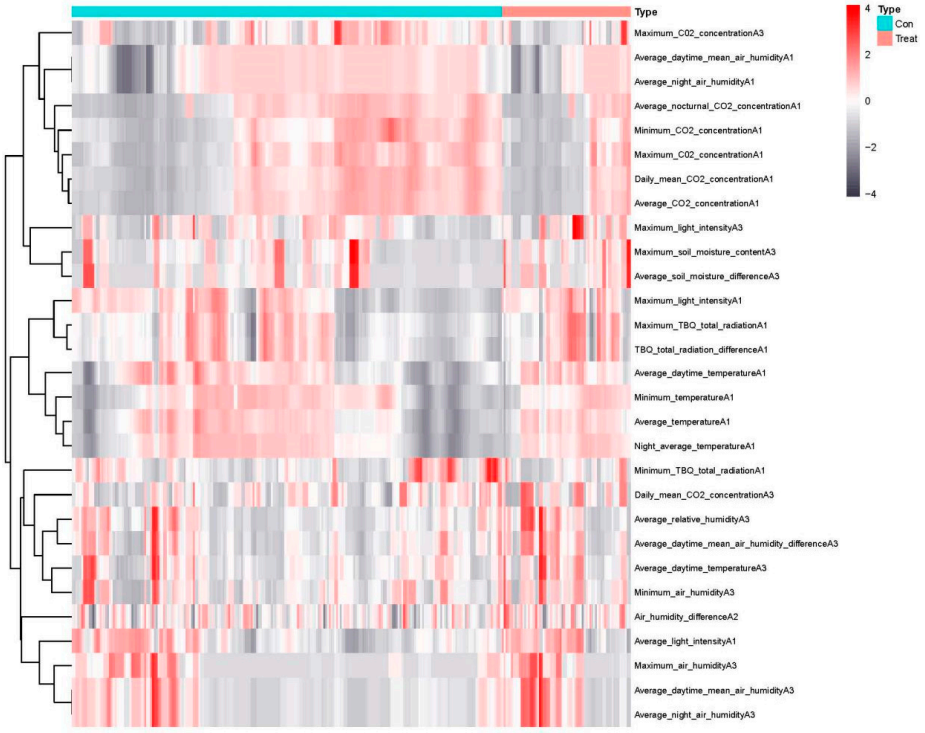


(**A**) Cluster Heatmap of Mild Diseases

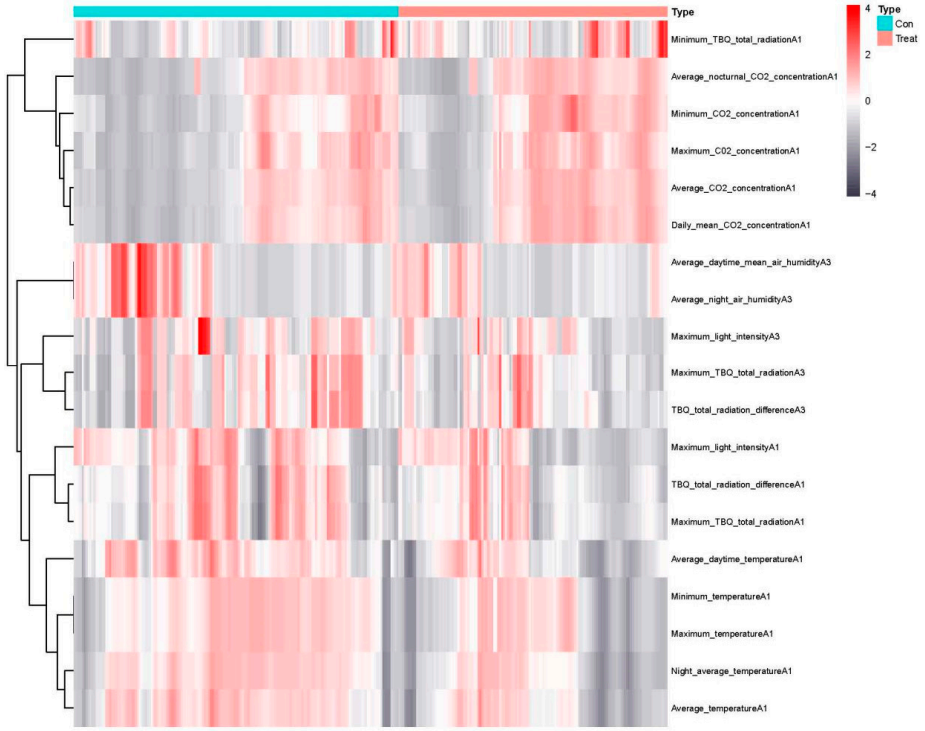


(**B**) Clustering Heatmap of Moderate Disease

**Figure 3.** *Cont.*

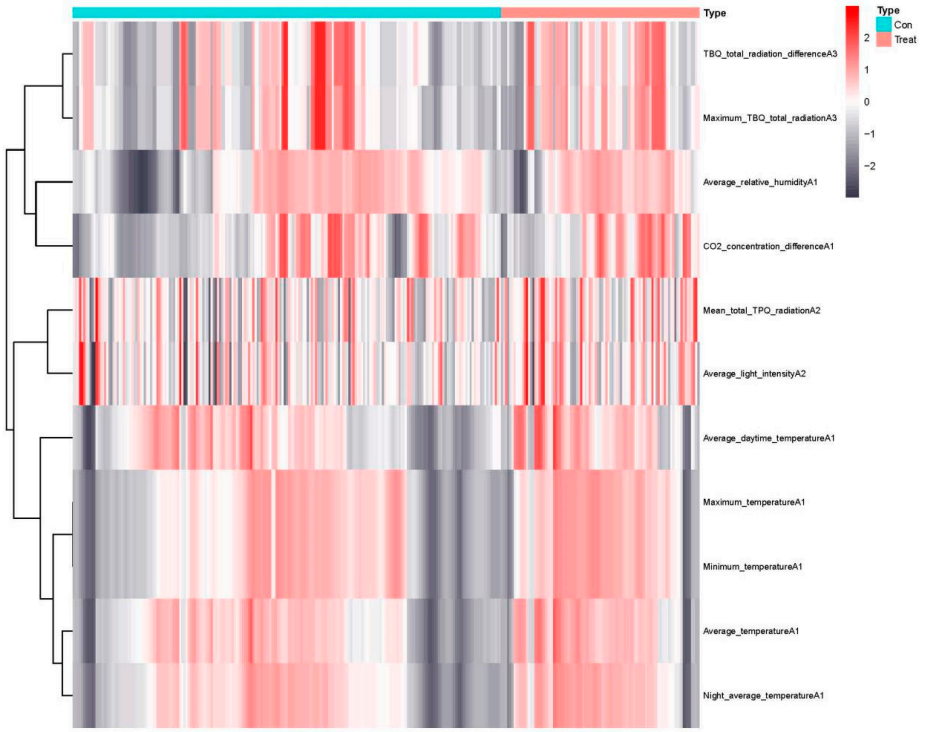


(**C**) Clustering Heatmap of Severe Disease

**Figure 3.** Clustering heatmap for diversity analysis.

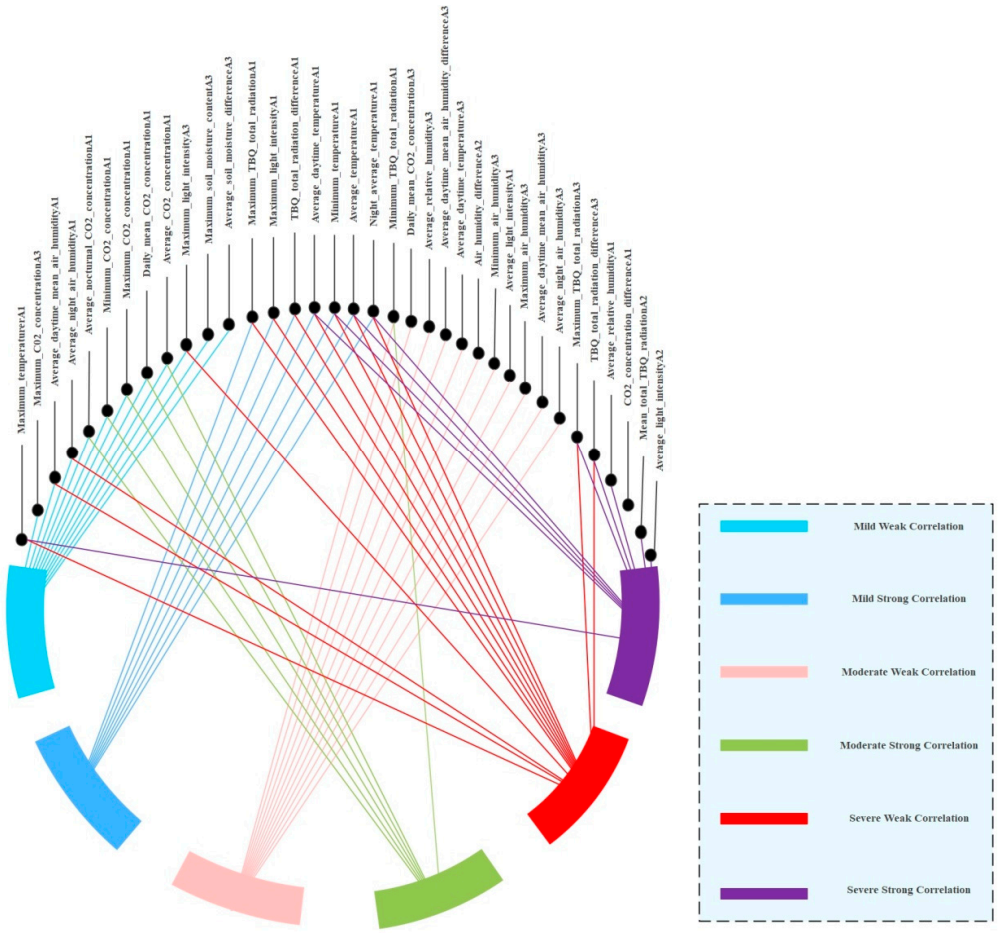


**Figure 4.** Correlation analysis (Cox univariate analysis).

### *3.3. Construction of LASSO-COX-NOMOGRAM Prediction Model*

The main idea of LASSO regression is to construct a first-order penalty function in order to obtain an accurate model. The complexity of LASSO is controlled by the parameter λ. As λ increases, the penalty for linear models with more variables also increases, resulting in the compression of some regression coefficients. This ultimately leads to the creation of a more accurate model with fewer variables. The LASSO loss function is represented by Equation (2):

$$L = \frac{1}{2m}[\sum_{i=1}^{m}\left(h_\theta\left(x^{(i)}\right) - y^{(i)}\right)^2 + \lambda\sum_{j=1}^{k}|w_j|] \quad (2)$$

where m represents the number of samples, k represents the number of parameters, and λ is the regularization parameter. The L1 regularization term is represented by $\lambda\sum_{j=1}^{k}|w_j|$. In LASSO regression, as the penalty coefficient increases, the coefficient gradually approaches zero, ultimately eliminating environmental factors weakly related to tea anthracnose.

Figure 5A shows the LASSO coefficient distribution, and 5B shows the cross-validation chart with Partial Likelihood Deviance on the *y*-axis and $\log(\lambda)$ on the *x*-axis. The dashed line on the left represents the minimum mean square error (lambda.min), and the dotted line on the right represents twice the error of the minimum mean square error (lambda.1se). In the experimental process, an ideal sparsity result is obtained by selecting an appropriate Lambda value, which provides a representative sparse representation of the Y value for the test sample. Bootstrap resampling and cross-validation methods are used to address the small sample size issue, ensuring reliable Lambda values. A total of nine modeling factors were identified, including average light intensity, maximum air humidity, minimum air humidity, average relative humidity, average daytime air humidity, average daytime carbon dioxide concentration, average nighttime carbon dioxide concentration, average total TBQ radiation, and maximum soil moisture content. Analysis results indicate that these nine factors significantly differ from tea anthracnose lesions ($p < 0.05$, Table 2).

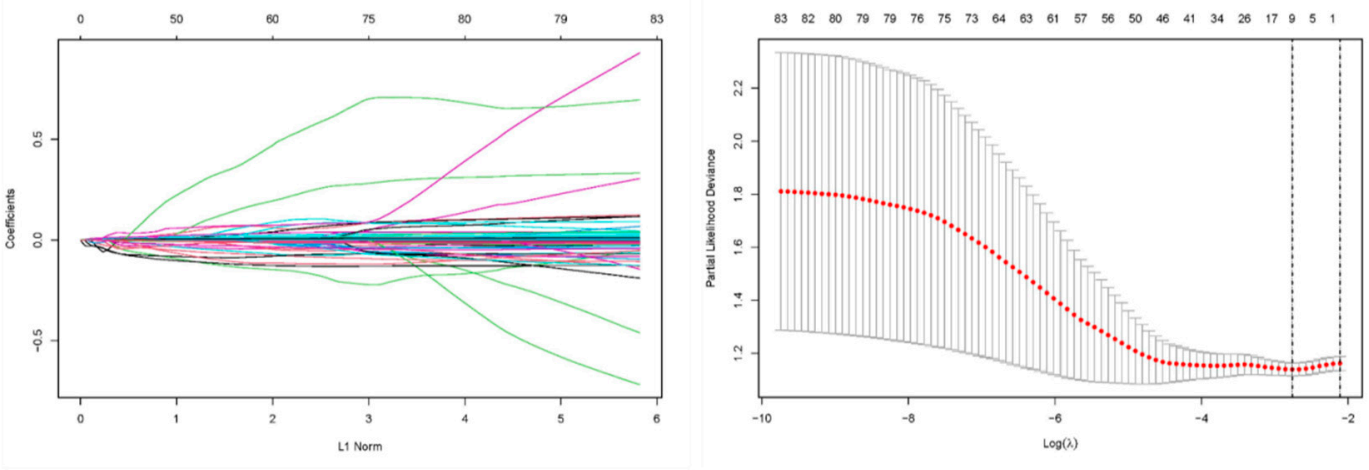


**Figure 5.** (**A**) Coefficient distribution in LASSO regression, and (**B**) cross-validation plot. Note: Different-color curves in (**A**) indicate different climate and environmental change factors in the same period. The left dashed line in (**B**) represents the minimum λ value. (**A**) shows the coefficient distribution in LASSO regression, and (**B**) shows the cross-validation plot.

In order to conduct Cox multi-factor analysis, we utilized 10-fold cross-validation to optimize the model. Additionally, we performed multiple linear regression analysis to verify the prediction results of all modeling factors on tea anthracnose lesions. The detailed results can be found in Table 4.

**Table 4.** Statistics of multivariate result statistics.

| Significant Environmental Correlation Factors | HR | CI | *p* |
|---|---|---|---|
| Average light intensity (A1.W) | 1.02 | 1.01–1.03 | 0.014 |
| Maximum air humidity (A2.W) | 1.34 | 1.11–1.61 | 0.002 |
| Minimum air humidity (A3.W) | 0.71 | 0.58–0.86 | 0.000 |
| Average relative humidity (A2.W) | 1.03 | 1.01–1.04 | 0.000 |
| Average daytime mean air humidity (A3.W) | 1.04 | 1.02–1.05 | 0.000 |
| Daily mean $CO_2$ concentration (A2.W) | 1.01 | 1.00–1.02 | 0.004 |
| Average nocturnal $CO_2$ concentration (A3.W) | 1.03 | 1.01–1.05 | 0.074 |
| Mean total TPQ radiation (A2.W) | 0.92 | 0.87–0.98 | 0.009 |
| Maximum soil moisture content (A2.W) | 2.01 | 1.27–3.18 | 0.003 |

Note: A1: mean value; A2: change difference; A3: change in floating value; W: 7 days; HR: Hazard Ratio; CI: Confidence Interval.

In order to further verify the necessity of the modeling factors screened by LASSO regression for model construction, an AIC analysis was performed. AIC is a standard for measuring the goodness of statistical model fitting. It is based on the concept of entropy and provides a trade-off estimate of model complexity. The criteria for the degree and goodness of fit to the data can be found in references [27–30]. The formula for AIC is as follows:

$$AIC = 2(p+1) - 2\ln L(\beta_1, \beta_2, \cdots \beta_n) \quad (3)$$

The greater the likelihood function value $L(\beta_1, \beta_2, \cdots \beta_n)$, the higher the probability of correct Cox classification and the greater the classification accuracy rate. In this case, there are often more unknown parameters $p+1$. The smaller the AIC value, the better the Cox regression model and the more reasonable the selection of the correct classification probability and complexity. It has been verified that the AIC value of the modeling factor screened by LASSO regression is 2809.033. This is a 24.2% reduction compared to the previous modeling factor with a strong correlation ($p < 0.05$), which had an AIC of 3705.08.

The nomogram is a visualization operation that utilizes multi-factor regression analysis to display the interrelationship between variables in a prediction model. It effectively represents the prediction weight of each modeling factor by drawing tick marks on the same plane according to a scale. The main concept behind this approach is to assign a score to each value of every modeling factor based on its predictive effect on tea plantation drought changes, as determined by the regression coefficient. This score is then transformed using a function that relates the total score to the probability of drought changes in tea gardens. Figure 6 illustrates the visualization results of the prediction model, including the names of the modeling factors, their scores, and the corresponding probabilities. The line segment scale following each modeling factor's name represents its value range, while the total length reflects its contribution to drought prediction. The score section comprises Point and Total Point, where Point signifies the individual score of each modeling factor under different values, and Total Point represents the cumulative score of all modeling factors. The analysis reveals that among all the modeling factors, maximum air humidity and maximum soil moisture have the most significant predictive effect on changes in tea anthracnose, whereas average relative humidity and maximum soil moisture content in the next 7 days have the least predictive effect. According to the research, the increase in air humidity will reduce the number of anthracnose spores to a certain extent, thus reducing the spread of anthracnose, which is similar to the research results of MacKenzie S J [31,32], Dragon DC [33–35], Ahsan M M, and other experts [36].

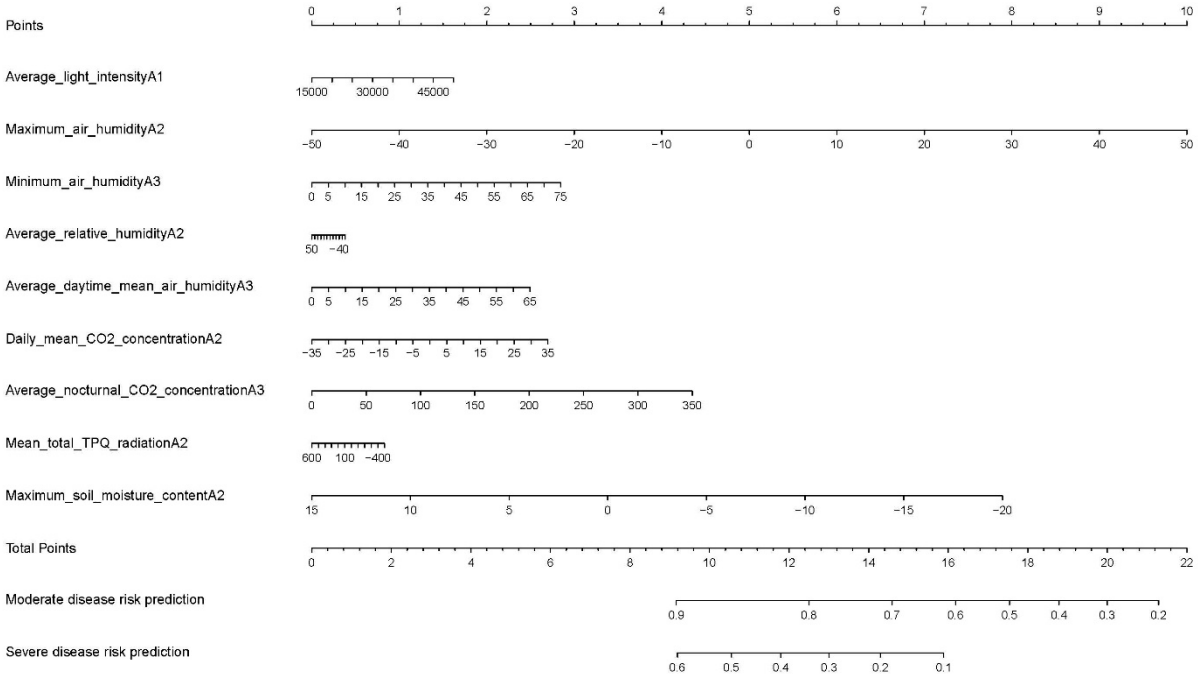


**Figure 6.** Prediction model of tea anthracnose disease change.

### *3.4. Verification of Model Discrimination*

This study utilized the ROC curve to analyze the accuracy of the risk score model in predicting the severity of disease following tea disease occurrence. Additionally, the ROC curve was employed to assess the discrimination ability of the LASSO-COX-NOMOGRAM prediction model. The efficiency of the model was evaluated through the ROC curve, with a larger area under the curve indicating a higher sensitivity and specificity of the model. Conversely, a smaller area suggests that the model lacks substantial significance. The survival ROC package in R software 4.1.2. was used to obtain the ROC curve, and the optimal cutoff point was determined based on maximum sensitivity and specificity. The Kaplan–Meier curve was then employed to evaluate the survival difference between low-risk and high-risk groups classified according to the optimal cutoff point. The Log-Rank test was utilized for further validation of the risk score formula by fitting the test set and validation set.

As demonstrated in Equations (4) and (5), this study categorizes the final results into two groups, Positive ($p$) and Negative (N), when assessing model discrimination. In terms of the consistency between the predicted value and the actual value, this study further divides the final results into True Positive (TP), False Negative (FN), False Positive (FP), and True Negative (TN). True Positive refers to cases where both the predicted value and the actual value of the disease degree change are positive examples. False Negative indicates that the model incorrectly predicts a positive example of disease degree change as a negative example. False Positive occurs when the model incorrectly predicts a negative example of disease degree change as a positive example. True Negative represents cases where both the predicted value and the actual value of the disease degree change are negative examples.

$$FPR = \frac{FP}{TN + FP} \tag{4}$$

$$TPR = \frac{TP}{TP + FN} \tag{5}$$

The ROC curve of the LASSO-COX-NOMOGRAM prediction model is presented in Figure 7. A higher discrimination of the prediction model is indicated by an ROC curve closer to the upper left corner. To further evaluate the model discrimination quantitatively,

this study introduces the AUC (area under the curve) index as a measure of the model's generalization performance. The AUC value directly reflects the generalization performance of the model, with a larger value indicating stronger generalization performance and discrimination. In statistical analysis, an AUC value greater than 0.7 is considered acceptable. In the LASSO-COX-NOMOGRAM prediction model, when the disease degree changes by more than 30%, the AUC value of the training set is 0.745 and the AUC value of the validation set is 0.75. For the situation where the disease degree changes by more than 60%, the AUC value of the training set is 0.731 and the AUC value of the validation set is 0.747 (Table 5). The results demonstrate that the AUC values of the LASSO-COX-NOMOGRAM prediction model for predicting changes in tea disease degree are all greater than 0.7, indicating good generalization performance and discrimination.

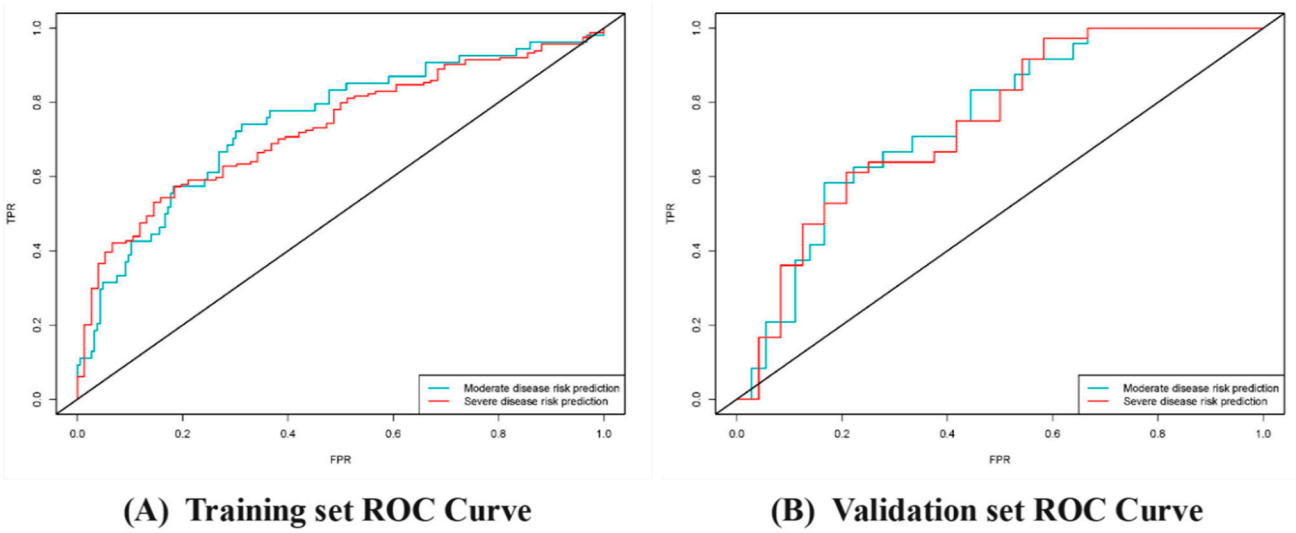


**Figure 7.** ROC curve of LASSO-COX-NOMOGRAM prediction model.

**Table 5.** Comparison of model discrimination.

| | Training Set AUC Value | Validation Set AUC Value |
|---|---|---|
| Moderate disease risk prediction | 0.745 | 0.75 |
| Severe disease risk prediction | 0.731 | 0.747 |

### *3.5. Verification of Model Calibration*

The calibration of a prediction model is a crucial indicator for evaluating the accuracy of a disease risk model in predicting the probability of future occurrence. It directly reflects the consistency between the model's predicted results and the actual outcomes. In order to assess the calibration, we performed Bootstrap resampling on the training set and validation set 1000 times. Figure 8 illustrates the calibration curves of the LASSO-COX-NOMOGRAM prediction model for changes in lesion extent exceeding 30% and 60%. Among these curves, A1 and B1 represent the calibration curves for changes in lesion extent greater than 30% and 60% in the training set, while A2 and B2 represent the calibration curves for changes in lesion extent greater than 30% and 60% in the validation set. The *X*-axis in this figure represents the predicted values of the LASSO-COX-NOMOGRAM model, while the *Y*-axis represents the actual values of the change in the degree of tea anthracnose lesions. The brown dotted line, with a slope of 1, indicates complete consistency between the actual and predicted risk changes. The red solid line represents the actual prediction ability of the LASSO-COX-NOMOGRAM model. The closer these two lines are to each other, the stronger the prediction accuracy. Within a statistical period, the two lines exhibit rough consistency.

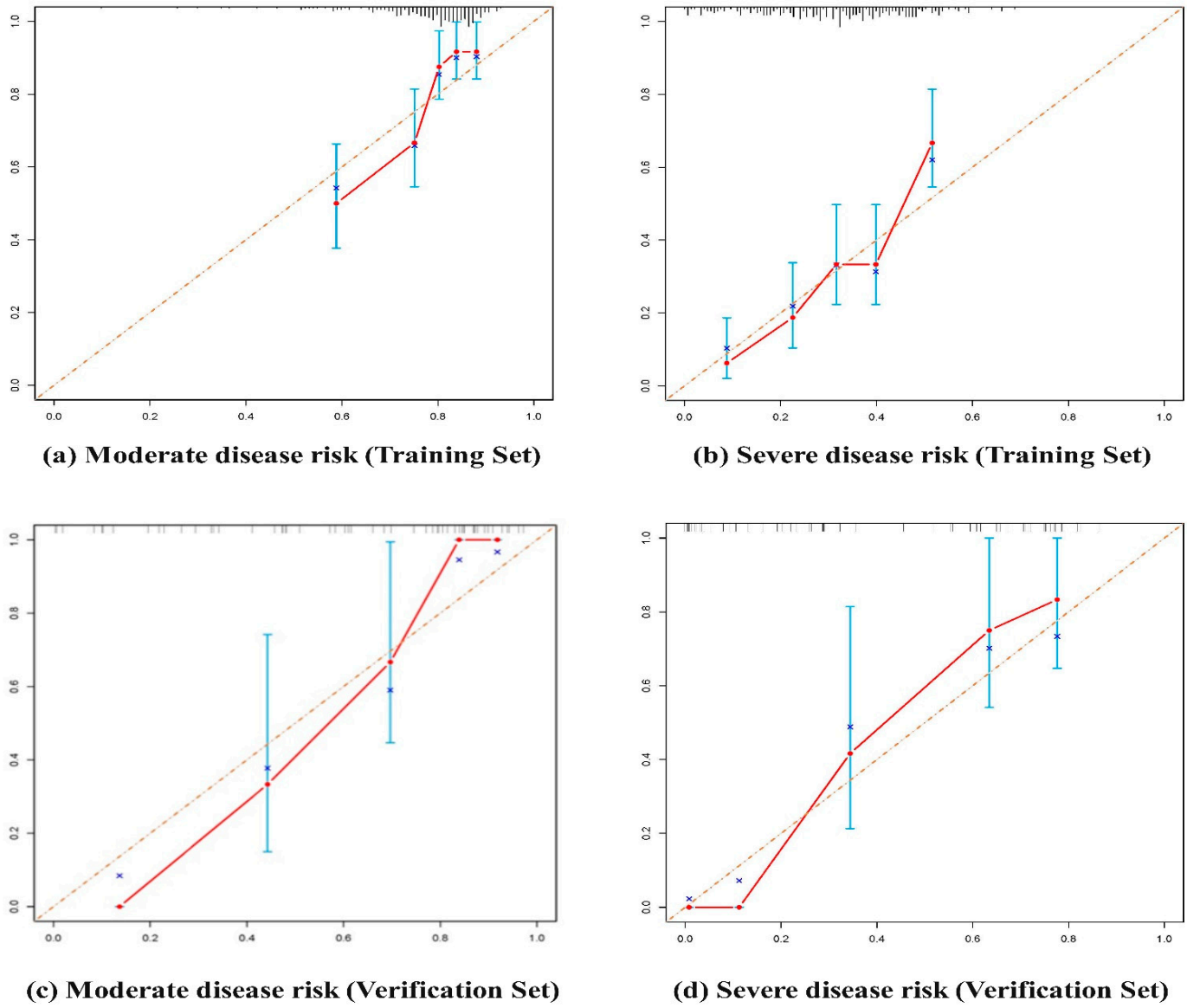


**Figure 8.** LASSO-COX-NOMOGRAM prediction model calibration curve. Red represents the actual calibration curve, and yellow dashed lines represent the ideal calibration curve.

### *3.6. System Development and External Verification*

By utilizing nomograms, complex regression equations can be transformed into more intuitive and readable graphics, thereby facilitating the evaluation of factors influencing diseases. To further enhance the ease of conducting risk prediction in real-life scenarios, this study adopts the Shiny framework and employs DynNOM technology to develop a visualization system for the prediction model. As depicted in Figure 9, the visualization system comprises five modules: the input module, Survival Plot, Predicted Survival, Numerical Summary, and Model Summary. The input module primarily handles data import and transformation. The Survival Plot illustrates the risk prediction probability of changes in environmental factors on tea disease levels. The Predicted Survival module presents the predicted comprehensive score for the disease in tabular form, while the Numerical Summary module displays it in numerical form. The Lesion comprehensive score is also showcased. Lastly, the Model Summary module is employed to adjust the modeling parameters of the risk prediction model. Figure 9a is used to visually show the lesion probability of tea anthracnose under different environmental changes. A lighter color means a lower prediction probability; Figure 9c clearly shows the detailed data of

each forecast, and the corresponding graphical display is shown in Figure 9b; Figure 9d contains all the parameters for building the prediction model.

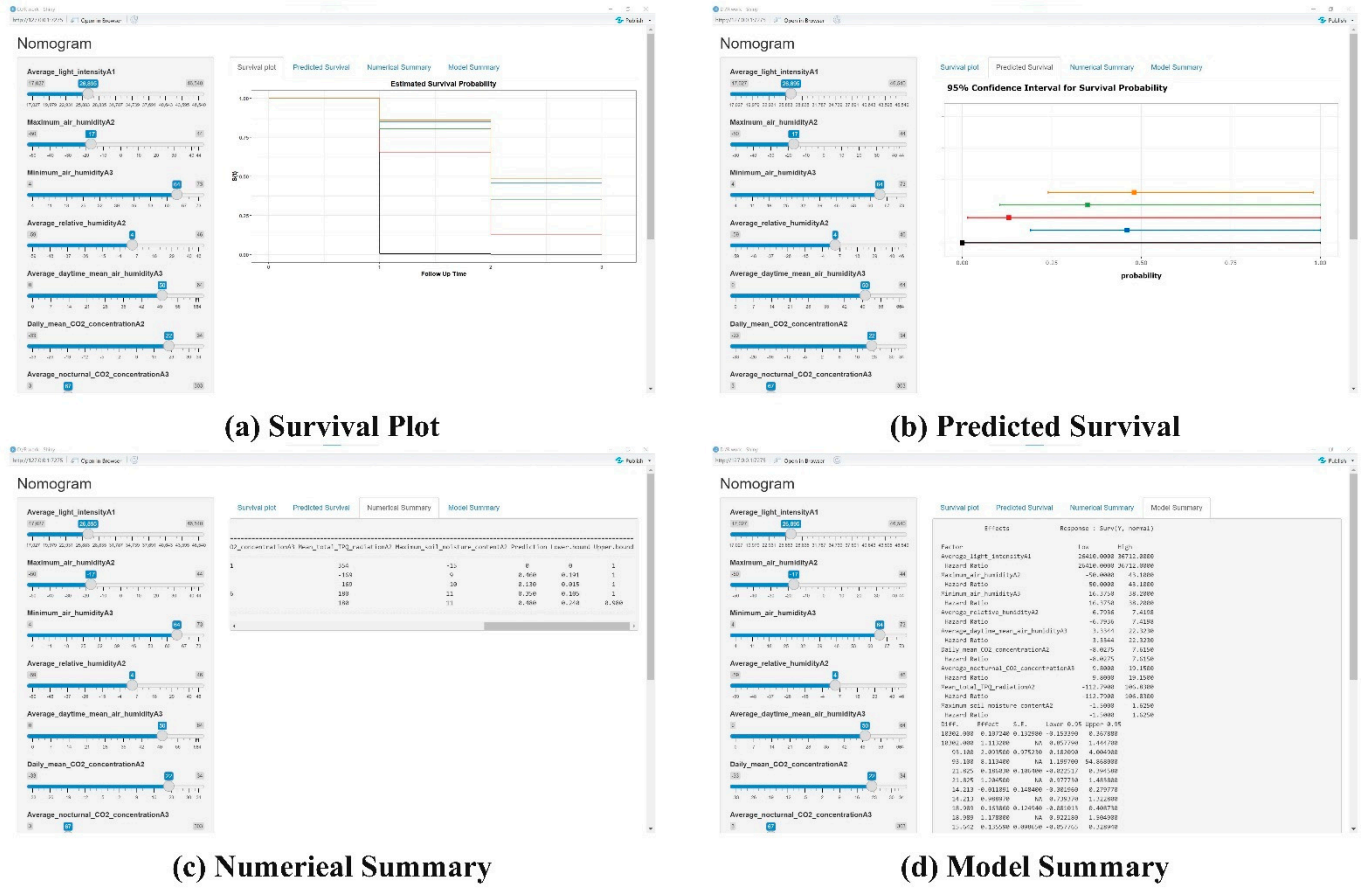


**Figure 9.** Prediction of tea disease system.

The environmental change data of Yuecheng Tea Garden Base in Xishuangbanna Prefecture, Yunnan Province, were collected through the Internet of Things in 2023 for model verification. The results are shown in Table 6, and the test results are shown in the table below. After testing the modeled data, if the comprehensive score falls between 0 and 0.2, the disease level will be low and the disease risk will be mild in the next 7 days. It is important to pay attention to protection measures and use biological control agents. If the comprehensive score falls between 0.2 and 0.6, the disease risk will be moderate in the next 7 days, and biodiversity technology should be applied. For example, acetone extracts from camphor leaves and mugwort can be used to inhibit the growth of tea anthracnose mycelium and spore germination. If the comprehensive score is greater than or equal to 0.6, the disease risk will be severe in the next 7 days, and infected tea leaves should be pruned to reduce the spread of the disease. The prediction result level aligns with the disease severity classification in Section 2.4 of this article. A total of 12 sets of data were tested for external verification, out of which 10 sets of prediction results were accurate and 2 sets were incorrect. The overall accuracy rate reached 83.3%, demonstrating the high reliability of the model in predicting tea disease risk. Compared to traditional logistic regression algorithm prediction, the Cox regression algorithm improved in accuracy by 16.6% after cross-validation and LASSO regression refinement in this study, with a significant improvement.

**Table 6.** Statistics of multivariate analysis results.

| Test Group | Comprehensive Score | Actual Result | Predicted Result | Yes/No | Logistic Regression Prediction |
|---|---|---|---|---|---|
| 1 | 0.840 | >0.6 | Three-Level | Yes | Three-Level |
| 2 | 0.800 | >0.6 | Three-Level | Yes | Three-Level |
| 3 | 0.610 | >0.6 | Three-Level | Yes | Three-Level |
| 4 | 0.566 | <0.6 | Three-Leve | No | Three-Level |
| 5 | 0.564 | 0.2–0.6 | Two-Level | Yes | Three-Level |
| 6 | 0.162 | <0.2 | Two-Level | No | Two-Level |
| 7 | 0.336 | 0.2–0.6 | Two-Level | Yes | Two-Level |
| 8 | 0.260 | 0.2–0.6 | Two-Level | Yes | One-Level |
| 9 | 0.091 | <0.2 | One-Level | Yes | One-Level |
| 10 | 0.090 | <0.2 | One-Level | Yes | One-Level |
| 11 | 0.100 | <0.2 | One-Level | Yes | One-Level |
| 12 | 0.127 | <0.2 | One-Level | Yes | One-Level |

## 4. Discussion

By considering the comprehensive influence of environmental change on the occurrence of tea anthracnose, the model provides valuable insights and predictions for further research on the impact of abiotic stress on the disease. One of the key contributions of this model is its potential to support decision making in the management of tea gardens. By offering data prediction and model support, it can enable tea garden managers to take proactive measures to prevent and control tea anthracnose. This is particularly important in regions like Yunnan, where tea production plays a significant role in the local economy.

Furthermore, the model's predictive capabilities have implications for the intelligent construction of tea gardens in specific regions of Yunnan. By considering the environmental factors that contribute to the risk of tea anthracnose, the model can guide the design and layout of tea gardens to minimize the impact of abiotic stress on the occurrence of the disease. The development of this risk degree prediction model can serve as a valuable tool for ongoing research on the impact of abiotic stress on tea anthracnose. The model's implications for tea garden management, intelligent construction, and ongoing research make it a valuable contribution to the field of tea anthracnose study and management. In the follow-up experiment, we will further consider the influence of soil pollution degree on the prediction of tea anthracnose incidence degree and incorporate it as a modeling factor in the prediction model construction.

## 5. Conclusions

This article investigates the short-term relationship between changes in disease within the tea garden ecosystem and environmental factors. A total of 21 environmental factors were analyzed, revealing significant correlations ($p < 0.05$). Notably, 90.5% of climate change factors were found to impact tea growth within the next 7 days. The risk of anthracnose also showed a significant association ($p < 0.01$). Additionally, an increase in carbon dioxide concentration, light intensity, TBQ radiation value, air temperature and humidity, and soil moisture during the change period was found to further escalate the risk of tea anthracnose.

Through LASSO, this study successfully identified nine crucial modeling factors after compressing and screening the data. These factors include average light intensity (average value), maximum air humidity (change difference), minimum air humidity (change in floating value), average relative humidity (change difference), average daytime air humidity (change difference), average daily $CO_2$ concentration (change difference), average nighttime $CO_2$ concentration (change difference), average total TBQ radiation (change difference), and maximum soil moisture (change difference). All of these modeling factors exhibit a significant relationship with disease changes ($p < 0.05$, Table 4).

The LASSO-COX-NOMOGRAM disease prediction model was tested and found to have an AUC value of 0.745 for the training set and 0.75 for the validation set when the

disease degree changes by more than 30% and 60%, respectively. Furthermore, the AUC value of the training set was 0.731 and the AUC value of the validation set was 0.747 in this scenario, indicating good generalization performance and discrimination of the model. The calibration curve demonstrated a high level of agreement with the ideal curve during the verification of model calibration, highlighting the strong prediction accuracy of the model. Additionally, when evaluating the accuracy of the LASSO-COX-NOMOGRAM drought prediction model and prediction system in different years, this research achieved an external verification accuracy rate of 83.3%.

This study provides valuable insights into the short-term disease risks of tea gardens. By accurately predicting these risks, it helps to improve the ecological balance and soil quality of tea gardens. Furthermore, the research results support the promotion of sustainable development through the implementation of eco-friendly management practices. This study can greatly enhance the long-term health and productivity of tea gardens, ultimately further improving the quality and yield of tea leaves.

**Author Contributions:** R.Y.: Conceptualization, Methodology, Software, Validation, Formal Analysis, Writing—Original Draft Preparation, Visualization. G.S.: Conceptualization, Methodology, Formal Analysis, Visualization. Z.M.: Conceptualization, Methodology, Writing—Review and Editing, Supervision. Q.G.: Formal Analysis, Visualization. B.W.: Conceptualization, Writing—Review and Editing. T.L.: Conceptualization, Supervision, Project Administration, Writing—Review and Editing, Funding Acquisition. All authors have read and agreed to the published version of the manuscript.

**Funding:** This research was funded by development and demonstration of the Yunnan Provincial Major Science and Technology Special Program Project-Integrated Research on Key Technologies of Smart Agriculture (202302AE090020), the Major Science and Technology Special Program of Yunnan Province-Construction of Crop Growth Model and Intelligent Control of Field (202202AE09002103), the Yunnan Provincial Basic Research Program-Research on Information Security Risk Analysis and Processing Methods for Smart Agriculture (202201AT070981), the Yunnan Provincial Science and Technology Talent and Platform Program-Yunnan Provincial Key Laboratory of Crop Production and Smart Agriculture (202105AG070007), and the General Project of Agricultural Basic Research Joint Special Program of Yunnan Province (Grant no. 202101BD070001-081).

**Data Availability Statement:** The original contributions presented in this study are included in this article. Further inquiries can be directed to the corresponding author.

**Acknowledgments:** We thank the editors and the anonymous reviewers for their valuable comments and suggestions.

**Conflicts of Interest:** The authors declare no conflicts of interest.

## References

1. Chaliha, C.; Kalita, E. Blister blight disease of tea: An enigma. In *Diagnostics of Plant Diseases*; InTech Open: London, UK, 2020.
2. Akintayo, A.; Tylka, G.L.; Singh, A.K.; Ganapathysubramanian, B.; Singh, A.; Sarkar, S. A deep learning framework to discern and count microscopic nematode eggs. *Sci. Rep.* **2018**, *8*, 9145. [CrossRef] [PubMed]
3. Bock, C.H.; Poole, G.H.; Parker, P.E.; Gottwald, T.R. Plant Disease Severity Estimated Visually, by Digital Photography and Image Analysis, and by Hyperspectral Imaging. *Crit. Rev. Plant Sci.* **2010**, *29*, 59–107. [CrossRef]
4. Naik, H.S.; Zhang, J.; Lofquist, A.; Assefa, T.; Sarkar, S.; Ackerman, D.; Singh, A.; Singh, A.K. A real-time phenotyping framework using machine learning for plant stress severity rating in soybean. *Plant Methods* **2017**, *13*, 23. [CrossRef] [PubMed]
5. Zhang, J.; Naik, H.S.; Assefa, T.; Sarkar, S.; Reddy, R.V.C.; Singh, A.; Singh, A.K. Computer vision and machine learning for robust phenotyping in genome-wide studies. *Sci. Rep.* **2017**, *7*, srep44048. [CrossRef] [PubMed]
6. Luo, Y.-H.; Jiang, P.; Xie, K.; Wang, F.-J. Research on optimal predicting model for the grading detection of rice blast. *Opt. Rev.* **2019**, *26*, 118–123. [CrossRef]
7. Bing, L.; Sun, J.; Yang, N.; Wu, X.; Zhou, X. Identification of tea white star disease and anthrax based on hyperspectral image information. *J. Food Process Eng.* **2021**, *44*, e13584. [CrossRef]
8. Kang, L.; Yuan, J.Q.; Gao, R.; Kong, Q.M.; Jia, Y.J.; Su, Z.B. Early Identification of Rice Leaf Blast Based on Hyperspectral Imaging. *Spectrosc. Spectr. Anal.* **2021**, *41*, 898–902. [CrossRef]

9. Nagasubramanian, K.; Jones, S.; Singh, A.K.; Sarkar, S.; Singh, A.; Ganapathysubramanian, B. Plant disease identification using explainable 3D deep learning on hyperspectral images. *Plant Methods* **2019**, *15*, 98. [CrossRef] [PubMed]
10. Huang, S.; Sun, C.; Qi, L.; Ma, X.; Wang, W. Rice panicle blast identification method based on deep convolution neural network. *Trans. Chin. Soc. Agric. Eng.* **2017**, *33*, 169–176.
11. Zhang, X.; Han, L.; Dong, Y.; Shi, Y.; Huang, W.; Han, L.; González-Moreno, P.; Ma, H.; Ye, H.; Sobeih, T. A Deep Learning-Based Approach for Automated Yellow Rust Disease Detection from High-Resolution Hyperspectral UAV Images. *Remote Sens.* **2019**, *11*, 1554. [CrossRef]
12. Wang, Y.C.; Yang, Y.J.; Xiao, B. Phylogenetic study of Colletotrichum species associated with Camellia sinensis from the major tea areas in China. *Sci. Agric. Sin.* **2015**, *48*, 4924–4935. [CrossRef]
13. Chen, Z.M.; Sun, X.L.; Dong, W.X. Genetics and chemistry of the resistance of tea plant to pests. In *Global Tea Breeding*; Springer: Berlin/Heidelberg, Germany, 2012.
14. Yu, G.; Wang, H.; Mo, Z.M.; Chen, F. Rhizome Quality Characteristics of Polygonatum rhizoma in Different. *J. Henan Agric. Sci.* **2023**, *52*, 57–68. [CrossRef]
15. Li, R.; Gong, Z.L.; Ye, C.P. Correlation between Environmental Factors and DownyMildew of Foxtail Millet. *Shaanxi J. Agric. Sci.* **2023**, *69*, 95–97. [CrossRef]
16. Li, R.G.; Jiang, Y.P.; Ding, X.T. Physiological and Ecological Analysis of Modern Greenhouse Cucumbers and Correlation of Environmental Factors. *Mol. Plant Breed.* **2024**, 1–12. Available online: https://kns.cnki.net/kcms/detail/46.1068.S.20230414.1601.004.html (accessed on 14 June 2024).
17. Li, Z.J.; Yu, G.D.; Liu, Q.; Zhang, Z.; Huang, J.; Liu, C.; Zhang, Q.; Chen, J. Effects of environmental factors and maize growth on surface temperature to monitor soil water content. *Trans. Chin. Soc. Agric. Eng.* **2022**, *38*, 77–85. Available online: http://www.tcsae.org/10.11975/j.issn.1002-6819.2022.20.009 (accessed on 14 June 2024). (In Chinese).
18. Dassanayake, M.K.; Khoo, T.J.; An, J. Antibiotic resistance modifying ability of phytoextracts in anthrax biological agent *Bacillus anthracis* and emerging superbugs: A review of synergistic mechanisms. *Ann. Clin. Microbiol. Antimicrob.* **2020**, *20*, 79. [CrossRef] [PubMed]
19. Chiaverini, A.; Abdel-Glil, M.Y.; Linde, J.; Galante, D.; Rondinone, V.; Fasanella, A.; Cammà, C.; D'Alterio, N.; Garofolo, G.; Tomaso, H. Whole Genome Sequencing for Studying *Bacillus anthracis* from an Outbreak in the Abruzzo Region of Italy. *Microorganisms* **2020**, *8*, 87. [CrossRef] [PubMed]
20. Wang, S.; Suluku, R.; Jalloh, M.B.; Samba, A.F.; Jiang, B.; Xie, Y.; Harding, D.; Zhang, M.; Sahr, F.; Sesay, M.E.; et al. Molecular characterization of an outbreak-involved Bacillus anthracis strain confirms the spillover of anthrax from West Africa. *Infect. Dis. Poverty* **2024**, *13*, 6. [CrossRef] [PubMed]
21. Yang, F.; Wang, W.; Wu, Z.; Xu, H.; Ge, M.; Lin, S.; Li, X.; Zhnag, Y.; Wu, C. Effects of Soil Nutrientand Measurement Ratioon Bacterial Community Structurein Fujian Tea Garden. *Ournal. Soil Water Conserv.* **2023**, *37*, 209–218. [CrossRef]
22. He, M.X. Study on biological characteristics of Colletotrichum camellia. *J. Zhejiang Agric. Sci.* **2005**, *4*, 316–318. [CrossRef]
23. Liu, W.; Chen, Y.S.; Liu, W.; Lian, L.L.; Zhu, Y.H.; Ye, N.X.; Wei, R.F. Effect of vacuum annealing on SERS spectra of Ag nanoparticle films deposited on AAO templates. *J. Ningde Norm. Univ.* **2013**, *25*, 1–5. [CrossRef]
24. Wilkinson, L.; Grimsrud, A.; Hughes, J.; Reuter, A.; Conradie, F.; Boyles, T. Critical changes to services for TB patients during the COVID-19 pandemic. *Int. J. Tuberc. Lung Dis.* **2020**, *24*, 542–544. [CrossRef]
25. Xue, Q.L.; Bandeen-Roche, K.; Tian, J.; Kasper, J.D.; Fried, L.P. Progression of Physical Frailty and the Risk of All-Cause Mortality: Is There a Point of No Return? *J. Am. Geriatr. Soc.* **2021**, *69*, 908–915. [CrossRef] [PubMed]
26. Wong, A.C.; Devason, A.S.; Umana, I.C.; Cox, T.O.; Dohnalová, L.; Litichevskiy, L.; Levy, M. Serotonin reduction in post-acute sequelae of viral infection. *Cell* **2023**, *186*, 4851–4867. [CrossRef] [PubMed]
27. Yuan, L.; Yan, P.; Han, W.Y.; Huang, Y.B.; Wang, B. Detection of anthracnose in tea plants based on hyperspectral imaging. *Comput. Electron. Agric.* **2019**, *167*, 105039. [CrossRef]
28. Liao, H.Z.; Liao, W.J.; Zou, D.X.; Zhang, R.Q.; Ma, J.L. Identification and expression analysis of PUB genes in tea plant exposed to anthracnose pathogen and drought stresses. *Plant Signal. Behav.* **2021**, *16*, 12. [CrossRef]
29. Anburaj, J.; Tamilselvi, E.; Chen, X.; Zhuang, J.; Wang, Y.H.; Li, X.H. Advances in understanding the mechanism of resistance to anthracnose and induced defence response in tea plants. *Mol. Plant Pathol.* **2023**, *24*, 1330–1346. [CrossRef]
30. Hu, G.S.; Wu, H.Y.; Zhang, Y.; Wan, M.Z. A low shot learning method for tea leaf's disease identification. *Comput. Electron. Agric.* **2019**, *163*, 104852. [CrossRef]
31. Peres, N.A.; Mackenzie, S.J.; Peever, T.L.; Timmer, L.W. Postbloom fruit drop of citrus and key lime anthracnose are caused by distinct phylogenetic lineages of *Colletotrichum acutatum*. *Phytopathology* **2008**, *98*, 345–352. [CrossRef]
32. MacKenzie, S.J.; Peres, N.A. Use of leaf wetness and temperature to time fungicide applications to control anthracnose fruit rot of strawberry in Florida. *Plant Dis.* **2012**, *96*, 522–528. [CrossRef]
33. Dragon, D.C.; Rennie, R.P. The ecology of anthrax spores: Tough but not invincible. *Can. Vet. J.* **1995**, *36*, 295. [PubMed]
34. Dragon, D.C.; Elkin, B.T.; Nishi, J.S.; Ellsworth, T.R. A review of anthrax in Canada and implications for research on the disease in northern bison. *J. Appl. Microbiol.* **1999**, *87*, 208–213. [CrossRef] [PubMed]

35. Dragon, D.C.; Rennie, R.P.; Elkin, B.T. Detection of anthrax spores in endemic regions of northern Canada. *J. Appl. Microbiol.* **2001**, *91*, 435–441. [CrossRef]
36. Ahsan, M.M.; Rahman Khan, M.F.; Rahman, M.B.; Chowdhury, S.M.Z.H.; Parvej, M.S.; Jahan, M.; Nazir, K.H.M.N.H. Investigation into Bacillus anthracis spore in soil and analysis of environmental parameters related to repeated anthrax outbreak in Sirajganj, Bangladesh. *Thai J. Vet. Med.* **2013**, *43*, 449–454. [CrossRef]

**Disclaimer/Publisher's Note:** The statements, opinions and data contained in all publications are solely those of the individual author(s) and contributor(s) and not of MDPI and/or the editor(s). MDPI and/or the editor(s) disclaim responsibility for any injury to people or property resulting from any ideas, methods, instructions or products referred to in the content.